International Airgun Modeling Workshop

Validation of Source Signature and Sound Propagation Models - Dublin (Ireland), July 16, 2016 - Problem Description

Ainslie, Michael A.; Laws, Robert M.; Sertlek, H. Ozkan

DOI
10.1109/JOE.2019.2916956

Publication date
2019

Document Version
Final published version

Published in
IEEE Journal of Oceanic Engineering

Peer-Reviewed Technical Communication

International Airgun Modeling Workshop: Validation of Source Signature and Sound Propagation Models—Dublin (Ireland), July 16, 2016—Problem Description

Michael A. Ainslie, Robert M. Laws, and H. Özkan Sertlek

***Abstract*—Computer models can be used to predict the sound field near an airgun or airgun array. The accuracy of such predictions can be assessed either by a process of verification (comparison with alternative theoretical solution to the same computational problem) or by validation (comparison with measurement). A set of verification test problems is described, as used originally by participants in the International Airgun Modeling Workshop held in Dublin, Ireland on July 16, 2016, and now by other authors in this special issue. The main inputs specified are the characteristics of the source (array geometry, airgun type and volume, and chamber pressure) and of the propagation medium (mainly water depth and bottom type). Also specified are source waveforms for individual airguns for authors wishing to focus only on the propagation aspects of the problem. The outputs are specified in terms of metrics derived from the sound pressure and sound particle acceleration.**

***Index Terms*—Airgun signature, propagation modeling, sound particle acceleration, sound pressure, source waveform.**

I. Introduction

A. Background

THIS paper forms part of a series of papers in the Special Issue on Verification and Validation of Airgun Source Signature and Sound Propagation Models [1]. It describes a set of test problems used by other contributors to this Special Issue. The same test cases–which require either the calculation of source waveform (signature model) or the sound field (propagation model) or both—were used previously in a 2016 modeling workshop held in Dublin, Ireland, summarized in [2]. Source waveforms were made available to authors wishing to focus on propagation.

Manuscript received April 30, 2018; revised January 10, 2019; accepted May 9, 2019. Date of publication June 7, 2019; date of current version July 12, 2019. The work was supported in part by the Netherlands Ministry of Infrastructure and the Environment, in part by the The E&P Sound & Marine Life Joint Industry Programme, in part by the National Oceanic and Atmospheric Administration, in part by the Bureau of Ocean Energy Management, and in part by the Acoustical Society of America. *(Corresponding author: Michael A. Ainslie.)*

Guest Editor: K. D. Heaney.

M. A. Ainslie was with TNO, 2597 AK, The Hague, The Netherlands. He is now with JASCO Applied Sciences (Deutschland) GmbH, Eschborn 65760, Germany, and also with the Institute of Sound and Vibration Research, University of Southampton, Southampton SO17 1BJ, U.K. (e-mail: michael.ainslie@jasco.com).

R. M. Laws was with Schlumberger Cambridge Research, Cambridge CB3 0EL, U.K. He is now with Havakustik Ltd., Cambridge CB4 1AJ, U.K (e-mail: laws@bcs.org.uk).

H. Ö. Sertlek is with the Faculty of Civil Engineering and Geosciences, TU Delft, 2628 CN Delft, The Netherlands, and also with the Electronics Engineering Department, Gebze Technical University, Gebze 41400, Turkey (e-mail: osertlek@gmail.com).

Digital Object Identifier 10.1109/JOE.2019.2916956

B. Terminology and Units

Airguns and sound propagation are specialized subjects, each with their own specialized jargons. If, in describing the test cases, we were to use the jargon of airgun sources, we would risk confusing propagation specialists and vice versa. At the risk of confusing both groups equally, instead we adopt a standard with international consensus, namely ISO 18405:2017 "Underwater Acoustics—Terminology" [3].

To avoid ambiguity, all parameters are specified in units compatible with the International System of Units (SI). Conversions to customary units, widely used to characterize airguns, follow IEEE 260.1-2004 "Letter Symbols for Units of Measurement (SI Customary Inch–Pound Units, and Certain Other Units)" [4]. Of particular interest in this regard are the pound–force per square inch, often abbreviated "psi," and the cubic inch. The psi (1 lbf/in^2) is a unit of pressure given by 1 lbf/in^2 $\approx$ 6895 Pa. The cubic inch (1 in^3) is a unit of volume given by 1 in^3 $=$ (25.4 mm)^3 $\approx$ 0.016387 L.

C. Content and Structure

The purpose of this paper is to specify a series of test problems involving the calculation of the sound field resulting from the use of an airgun or airgun array in shallow water. The coordinate systems used are specified in Section II. The airgun sources and the propagation medium are described in Sections III and IV, respectively, followed by a list of four test problems (see Section V) and some closing remarks (see Section VI).

II. Coordinate Systems

Three different coordinate systems are used as follows.

A. Cartesian (x, y, z)

Cartesian coordinates are used to specify the geometry of the source arrays. A right-handed Cartesian coordinate system is adopted with x increasing ahead, y increasing to starboard, and z increasing downward. The spatial origin is at the sea surface.

B. Cylindrical Polar (r, z, ϕ)

Cylindrical polar coordinates are used to specify receiver positions: $z =$ depth from sea surface, $r =$ horizontal distance from origin, and $\phi =$ bearing clockwise from the x-axis looking down (clockwise from straight ahead in plan view). The spatial origin is at the sea surface (in the same position as for the Cartesian coordinates). Conversion to

TABLE I
SOURCES S1, S2, AND S3

Source parameter	S1	S2	S3
Array length	N/A	15 m	15 m
Sub-array separation	N/A	N/A	15 m
Source depth	5 m	5 m	See Table VI
Nominal total source volume	155 in^3 (2.5 L)	1315 in^3 (21.5 L)	3333 in^3 (54.6 L)
Airgun type	Bolt 1500LL	Bolt 1500LL and 1900LLX	Bolt 1500LL and 1900LLX
Nominal chamber pressure	2000 lbf/in^2 (13 790 kPa)	2000 lbf/in^2 (13 790 kPa)	2000 lbf/in^2 (13 790 kPa)
Notes	Third airgun of S2	Center sub-array of S3 (nominal positions)	

A source depth of 5 m is chosen to facilitate comparison with an equivalent problem [5] based on the 2010 Weston Modeling Workshop [6].

TABLE II
AIRGUN PROPERTIES FOR USE IN TEST CASES

Quantity	Definition	Exact value	Approximate conversions
Total air pressure (P_{tot})	Pressure of air inside airgun before firing	13 890.8 kPa	2015 lbf/in^2
Atmospheric pressure (P_{atm})	Pressure of water at the sea surface	101.3 kPa	15 lbf/in^2
Water temperature	Temperature of water surrounding airgun before firing	10 °C	
Inter-pulse interval	Reciprocal of firing repetition frequency	10 s	
Delay in firing time (all airguns)		0	

The interpulse interval (or repetition rate) affects the average airgun temperature [7].

TABLE III
SOURCE S1 CONFIGURATION

x / m	y / m	z / m	Airgun type	V / L
0.00	0.00	5.00	1500LL 155	2.540

TABLE IV
SOURCE S2 CONFIGURATION

x / m	y / m	z / m	Airgun type	V / L	Airgun number
+6	0.00	5.00	1500LL 480	7.866	S2G01
+3	0.00	5.00	1500LL 290	4.752	S2G02
0	0.00	5.00	1500LL 155	2.540	S2G03
−3	0.00	5.00	1900LLX 200	3.277	S2G04
−6	0.00	5.00	1900LLX 100	1.639	S2G05
−9	0.00	5.00	1900LLX 90	1.475	S2G06

The total array volume is 21.549 L (1315 cubic inches).

Cartesian coordinates are effected using

$$x = r\cos(\phi)$$
$$y = r\sin(\phi)$$
$$z = z.$$

C. Spherical Polar (θ, ϕ)

Spherical polar coordinates are used to characterize the directional dependence of the source signature (the source waveform of an airgun array varies with bearing and elevation): θ is the elevation angle increasing downward from horizontal and ϕ is the bearing angle defined in the same way as in cylindrical coordinates.

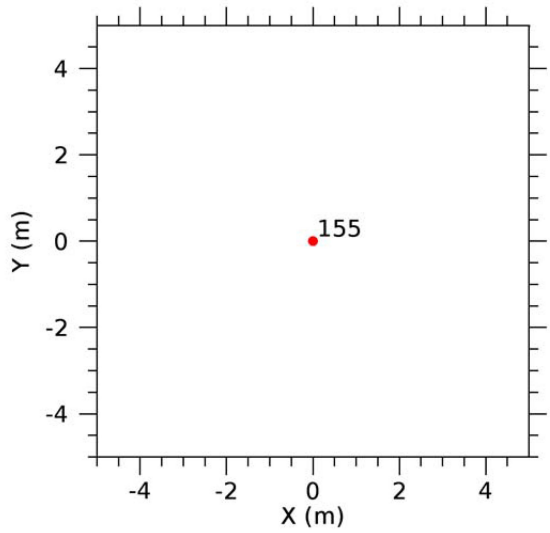

Fig. 1. Source S1 is situated directly beneath the origin.

III. SOURCE SPECIFICATION

A. Overview

Three different sources are considered, denoted by "S1" to "S3." These are a single Bolt 1500LL airgun (S1), a single line array of six airguns, including S1 (S2), and an array comprising three subarrays, including S2 as the center subarray (S3) (see Table I).

For purposes of identification, Table I uses customary units, as conventionally used by airgun suppliers. In the rest of this specification, SI units are followed, with an approximate conversion to customary units in brackets where appropriate. Airgun properties common to all three sources are specified in Table II.

The density of water and the acceleration due to gravity are specified to be $\rho = 1000$ kg/m^3 and $g = 9.81$ m/s^2, respectively. Using these values, the following properties follow from Table II:

1) the water pressure at depth $z = 5$ m is $P_{\text{w}} = P_{\text{atm}} + \rho g z = 150.4$ kPa (22 lbf/in^2);
2) the chamber (or gauge) pressure $(P_{\text{g}} = P_{\text{tot}} - P_{\text{atm}})$ is 13 789.5 kPa (2000 lbf/in^2);
3) the airgun pressure relative to the hydrostatic pressure $(P_{\text{tot}} - P_{\text{w}})$ is 13 740.5 kPa (1993 lbf/in^2).

The source description includes signatures calculated using Agora [8]. These signatures (source waveforms) form part of the problem description and were made available to authors wishing to focus on propagation aspects. The Agora input files and source code are available from the Ocean Acoustics Library [9]. The corresponding source waveforms are available from IEEE Dataport [10].

B. Choice of Spatial and Temporal Origins

For all sources, the spatial origin is at the sea surface. For S1, it is directly above the airgun; for S2, it is directly above the third airgun (S2G03); and for S3, it is directly above the third airgun in the center array (S3G09).

For S1, participants are requested to select and specify a time origin of their own choices. For S2 and S3, the airguns are nominally fired simultaneously. In a commercial airgun array, there is typically an

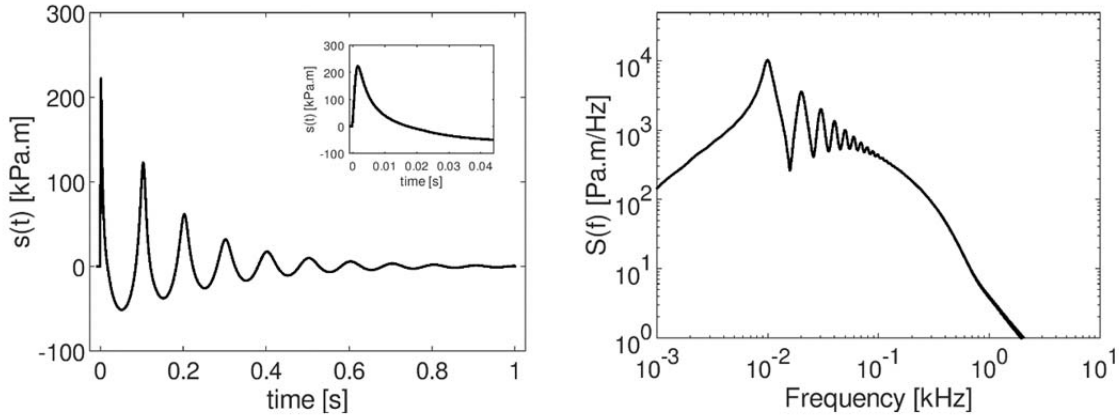

Fig. 2. S1 source waveform $s(t)$ (left) and the magnitude of its spectrum $|S(f)|$ (right).

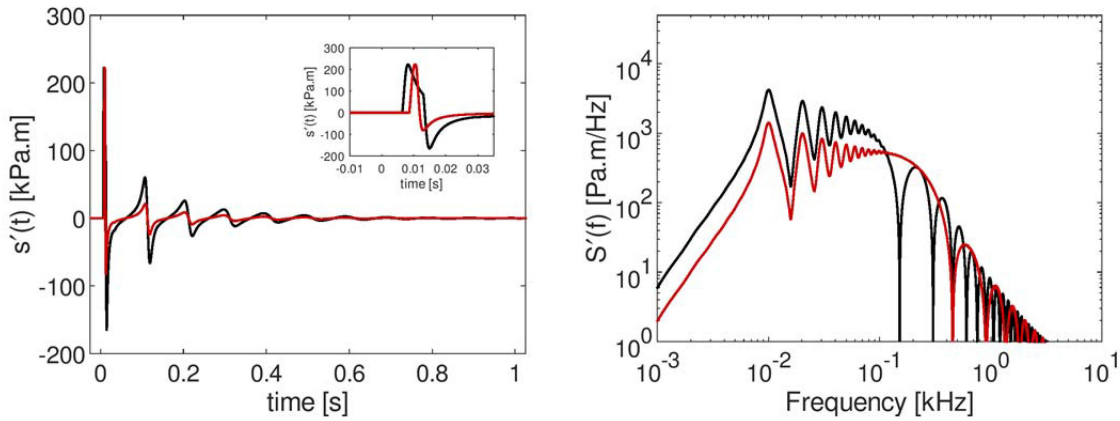

Fig. 3. S1 surface-affected source waveforms $s'(t)$ (left) and the magnitude of their spectra $|S'(f)|$ (right). The elevation angles (θ) are 20° (red) and 90° (black) from horizontal.

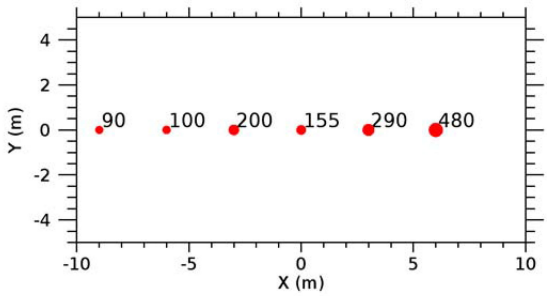

Fig. 4. Plan view of source S2 layout. The source is at $y = 0$ and is towed toward the right.

automatic adjustment of the timing of the firing pulses. This is done to synchronize the actual onset of the main pressure pulses. The time delay between the firing pulse and the airgun acoustic pulse onset usually varies between airguns in the array, but it is approximately constant for each airgun.

Before the main pulse is emitted, there can be various acoustic precursors that result from the initial movement of mechanical parts and the fluid flows. Airgun modeling codes often include these precursor signals in some way, but they are not used in the synchronization process.

To represent the synchronization process in a simple way with the modeled data, the notional sources have been synchronized by time shifting them after simulation such that the pulse onsets are simultaneous. To do this without the precursor signals upsetting the calculation, the pulse onset is deemed to start when the source waveform reaches a value of 20 kPa·m, and the time origin has been chosen to ensure that this onset occurs at a time of 10 ms for each notional source. This value is small enough to correspond with the onset of the pulse while large enough to not be triggered by the precursor.

C. Source S1

S1 (see Table III) is the third airgun from source S2 (see Table IV). The spatial origin is at the sea surface, directly above the airgun. See also Fig. 1.

The source waveform $s(t)$ for source S1 and the magnitude of the corresponding source spectrum $|S(f)|$ are plotted in Fig. 2. The source waveform is sometimes referred to as the "notional source signature" [11]–[13].

The source spectrum $S(f)$ is the Fourier transform of $s(t)$ [3]

$$S(f) = \int_{-\infty}^{+\infty} s(t) \exp(-2\,\pi i\; ft) dt. \tag{1}$$

The corresponding energy source spectral density level $L_{S,E}$ can be defined in terms of the source spectrum using [8]

$$L_{S,E} \equiv 10 \lg \frac{2|S(f)|^2}{1\ \mu\text{Pa}^2 \cdot \text{m}^2 \cdot \text{s} \cdot \text{Hz}^{-1}}\ \text{dB}. \tag{2}$$

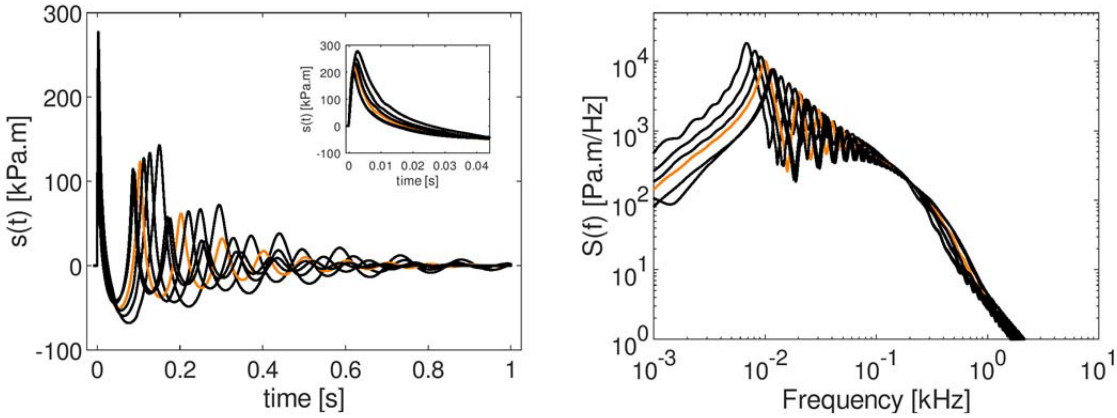

Fig. 5. Source waveforms $s(t)$ of the six S2 airguns (left) and the magnitude of their spectra $|S(f)|$ (right). The orange curve indicates the same airgun as S1.

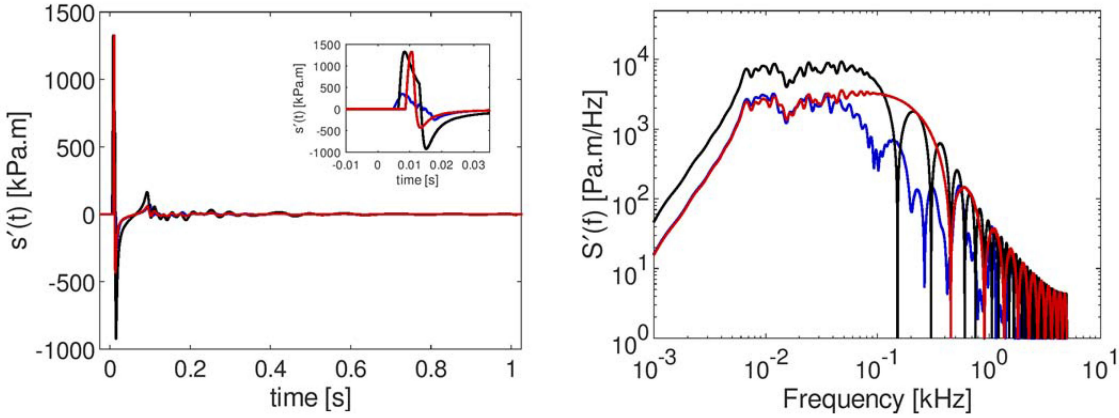

Fig. 6. S2 surface-affected source waveforms $s'(t)$ (left) and the magnitude of their spectra $|S'(f)|$ (right). The elevation angles (θ) are 20° [blue: straight ahead $(\phi = 0)$; red: broadside $(\phi = 90°)$] and 90° (black) from horizontal.

The factor 2 in (2) is needed to convert a double-sided spectral density into a single-sided one [3]. The reference value of 1 $\mu\text{Pa}^2 \cdot \text{m}^2 \cdot \text{s} \cdot \text{Hz}^{-1}$ is preferred over 1 $\mu\text{Pa}^2 \cdot \text{m}^2 \cdot \text{Hz}^{-2}$ (or 1 $\mu\text{Pa} \cdot \text{m} \cdot \text{Hz}^{-1}$) to emphasize the nature of $2|S(f)|^2$ as the spectral density of the energy source factor [3].

The surface-affected source waveform $s'(t)$ for source S1 and the magnitude of the corresponding surface-affected source spectrum $|S' + (f)|$ are plotted in Fig. 3. Before calculating these and other spectra, the time-domain signal is first padded with zeros for 10 s after the signal.

The surface-affected quantities include the contribution from the source's image ("ghost") in the sea surface, and the surface-affected source spectrum $S'(f)$ is the Fourier transform of $s'(t)$ [3]

$$S'(f) = \int_{-\infty}^{+\infty} s'(t) \exp(-2\,\pi i\; ft) dt. \tag{3}$$

The corresponding surface-affected energy source spectral density level $L_{S',E}$ can then be defined as

$$L_{S',E} \equiv 10 \log_{10} \frac{2|S'^{(f)}|^2}{1\ \mu\text{Pa}^2 \cdot \text{m}^2 \cdot \text{s} \cdot \text{Hz}^{-1}}\ \text{dB}\ . \tag{4}$$

TABLE V
SOURCE S3 CONFIGURATION

Source parameter	Value	Notes
Array length	15 m	
Sub-array separation	15 m	
Total source volume (V)	54.618 L	Nominal volume is 3333 in^3
Airgun type	Bolt 1500LL and 1900LLX	

D. Source S2

The geometry of S2 is illustrated by Fig. 4 and specified in Table IV. The spatial origin is at the sea surface, directly above the third airgun (S2G03, which is identical to S1).

The source waveforms and source spectra for each of the six S2 airguns are plotted in Fig. 5. The surface-affected source waveform and spectrum for the array are plotted in Fig. 6. Here and throughout, the Agora waveforms are aligned before any processing to pass through 20 kPa·m at 10 ms.

E. Source S3

The array chosen for S3 (see Table V) is the one used in a 2008 survey commissioned by Shell (EPE L09-FF 4D, September 23, 2008

TABLE VI
SOURCE S3 CONFIGURATION

Array component	x / m	y / m	z / m	Airgun type	V / L	Airgun number
Starboard (inner) sub-array	1.09 (+1)	15.01	4.74	1500LL 480	7.866	S3G01
	−2.17 (−2)	15.02	7.18	1500LL 290	4.752	S3G02
	−4.53 (−5)	14.18	6.91	1900LLX 200	3.277	S3G03
	−7.94 (−8)	14.82	5.75	1900LLX 125	2.048	S3G04
	−11.13 (−11)	14.79	6.14	1900LLX 100	1.639	S3G05
	−13.81 (−14)	15.56	5.73	1900LLX 54	0.885	S3G06
Sub-total					**20.467**	
Center sub-array	5.82 (+6)	0.21	6.21	1500LL 480	7.866	S3G07
	3.16 (+3)	0.37	5.76	1500LL 290	4.752	S3G08
	0.00 (0)	0.00	5.00	1500LL 155	2.540	S3G09
	−2.76 (−3)	−0.72	4.86	1900LLX 200	3.277	S3G10
	−6.10 (−6)	−1.62	6.11	1900LLX 100	1.639	S3G11
	−8.87 (−9)	−0.52	6.08	1900LLX 90	1.475	S3G12
Sub-total					**21.549**	
Port (outer) sub-array	−3.42 (−3)	−14.99	4.96	1500LL 290	4.752	S3G13
	−6.49 (−6)	−15.23	5.71	1900LLX 200	3.277	S3G14
	−9.27 (−9)	−14.59	4.96	1900LLX 125	2.048	S3G15
	−12.47 (−12)	−15.75	4.84	1900LLX 100	1.639	S3G16
	−15.49 (−15)	−14.38	5.01	1900LLX 54	0.885	S3G17
Sub-total					**12.602**	

Nominal x coordinates are indicated in brackets. Nominal y coordinates in meters are (+15, 0, −15) for starboard, center, and port arrays, respectively. Nominal z coordinates are 5 m for all airguns. The total array volume is 54.618 L (3333 cubic inches).

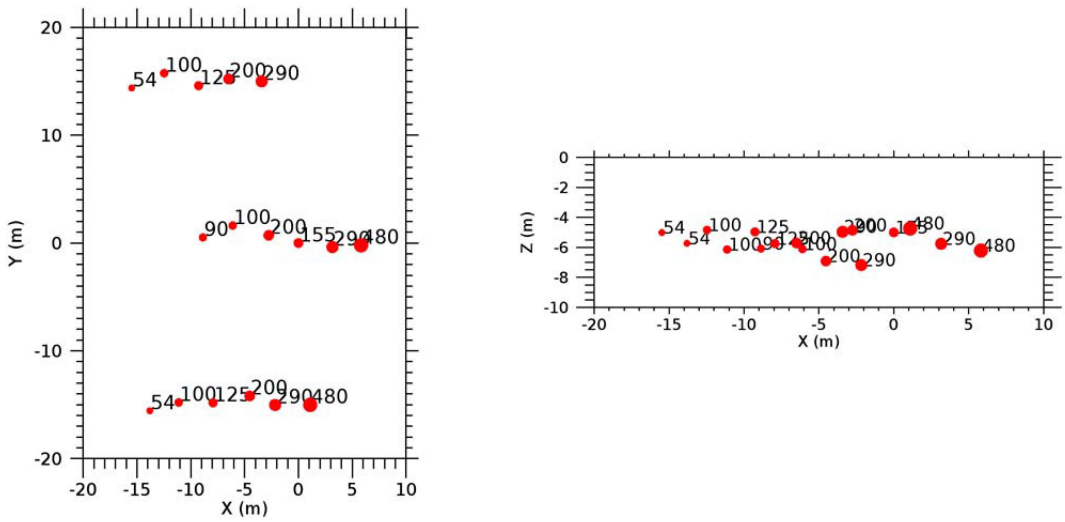

Fig. 7. Plan view (left) and side view (right) of source S3 layout. The source is towed toward the right.

to October 15, 2008; port array), using an array with a source depth of 5 m and no airgun clusters.

The geometry of S3 is specified in Table VI and illustrated by Fig. 7. The S3 airgun positions (see Table VI) include some random perturbations relative to the nominal positions (in brackets). The spatial origin is at the sea surface, directly above the third airgun of the center subarray (S3G09). To achieve this, after applying the random offsets from the position of all airguns, the entire array is shifted such that S3G09 is located at (0, 0, 5) m. The departures from the airguns' nominal positions are drawn from a Gaussian distribution. After application of the random offsets to the airguns from their nominal positions, S3G09 is at (0.86, 0.15, 4.61) m. The entire array is displaced by (−0.86, −0.15, +0.39) m to place S3G09 at (0, 0, 5) m precisely, leading to the coordinates of Table VI. Apart from the small random offsets from the nominal airgun positions, the center subarray is identical to S2.

The random perturbations in S3 are to prevent artificial coherent reinforcement of the airgun signal at high frequency. Similar perturbations could have been applied to S2 for the same reason, but it was preferred to keep this case simple to avoid unnecessary computational and logistical complexity in the step from S1 to S2.

Scatter in x (the standard deviation of the distribution around the nominal position) is 0.25 m. Scatter in y is 0.50 m. Scatter in z is 0.50 m. The distributions in x, y, and z are assumed Gaussian and uncorrelated.

Airgun bubbles interact with each other: each bubble is subjected not only to the ambient pressure, but also to the fluctuating sound pressure caused by the sound field radiated by other bubbles and their surface-reflected images. The interactions cause the emitted notional source waveform of a bubble to be modified compared with when it is fired alone. Because of the influence of surface reflections, this modification is needed even for a single airgun.

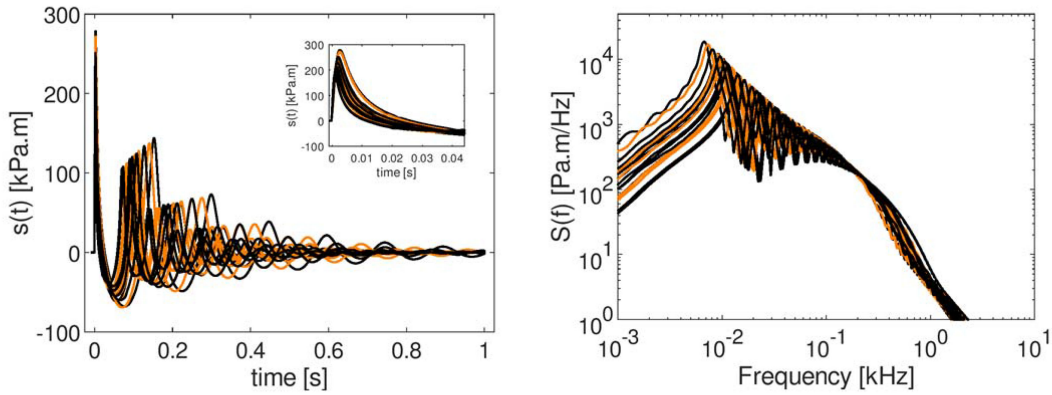

Fig. 8. Source waveform (left) and magnitude of its spectrum (right) of the 17 airguns of source S3. Orange curves indicate the same airguns as S2.

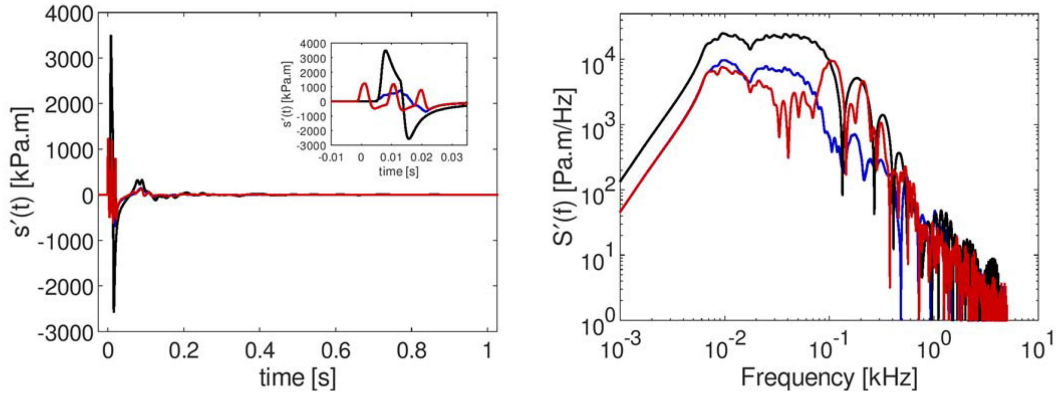

Fig. 9. S3 surface-affected source waveforms $s'(t)$ (left) and the magnitude of their spectra $|S'(f)|$ (right). The elevation angles (θ) are 20° [blue: straight ahead $(\phi = 0)$; red: broadside $(\phi = 90°)$] and 90° (black) from horizontal.

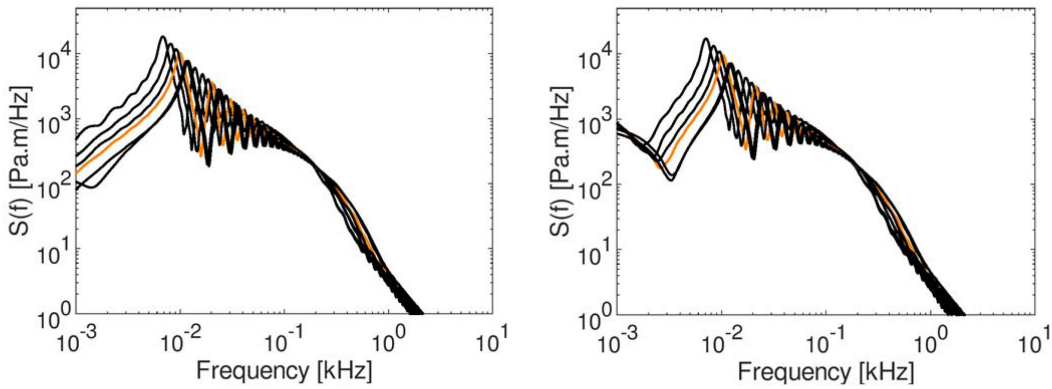

Fig. 10. Source spectra $|S(f)|$ of the six S2 airguns predicted using Agora-2 (left, repeated from Fig. 5) and Agora-1 (right). The orange curve indicates the same airgun as S1.

The source waveform and source spectra for the 17 airguns of the S3 source are plotted in Fig. 8. The surface-affected source waveform and corresponding spectra for the array are plotted in Fig. 9.

F. Source Waveform Model

1) Overview: Airgun sourcewaveforms were calculated using the Agora source signature model [8], available from the Ocean Acoustics Library [9]. These waveforms were made available to potential contributors to this special issue and placed in Dataport [10]. A set of differential equations involving the bubble radius is constructed including terms representing mass transfer, thermal effects, gas pressure laws, and momentum. Following [14], Agora applies Gilmore's equation and additionally includes mass and heat transfer [15], [16]. By means of a recursive solution of this differential equation system, Agora calculates the bubble radius, bubble wall velocity, temperature, and mass of the bubble. The radiated pressures from each airgun are then separately calculated from these parameters. Bubble interactions are added as a perturbation to the ambient pressure [17]. The state of the gas inside the airgun differs from that of the air bubble; the two states are linked by equations describing the flow of air through the airgun ports [15].

2) Agora-1 and Agora-2: Two versions of Agora data were supplied to authors. Agora-1 data were distributed in 2016, a few months

TABLE VII
MEDIUM PARAMETERS

Parameter	Water	Sediment	Notes
Sound speed	1500 m/s	1700 m/s	
Density	1000 kg/m^3	2000 kg/m^3	
Absorption coefficient	See Equation 5	0.2941 dB/(m kHz)	0.2941 dB/(m kHz) corresponds to 0.5 decibels per wavelength in the sediment (i.e., $\alpha\lambda = 0.5$ dB, often written as $\alpha = 0.5$ dB/λ)

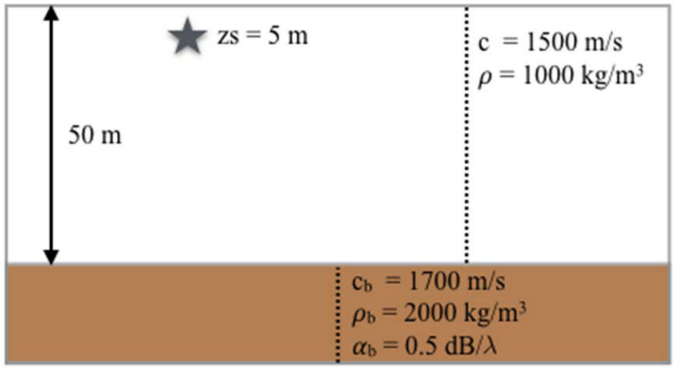

Fig. 11. Propagation medium. The seabed is perfectly smooth, with properties shown in Table VII (artwork by E. Küsel, with permission).

before the Dublin workshop [2]. Agora-2 data were made available in March 2018. The differences between these two data sets (see Fig. 10) are mainly associated with minor code changes. Further, an adjustment was made to the water temperature from 22.2 °C (used with Agora-1) to 10.0 °C (Agora-2). The tick in the right-hand graph at low frequency (<5 Hz) is caused by an error identified in Agora-1 that was corrected in Agora-2. The error appears in the S2 and S3 waveforms, but not in S1. Authors not using their own source waveform model were encouraged to use the Agora-2 data set, as available from IEEE Dataport [10].

IV. MEDIUM SPECIFICATION

The propagation medium (see Table VII and Fig. 11) is based on the 2010 Weston Memorial Workshop (WMW) [6], adapted for the shallow water problem (50-m water depth instead of 100 m) as described by Colin et al. [5]. The reason for choosing the WMW scenarios is that benchmark solutions exist for some cases of interest [18], [19].

The absorption coefficient of seawater as a function of frequency f follows [20]:

$$\frac{\alpha_{\text{water}}}{\text{Np}\cdot\text{km}^{-1}} = 1.40\times10^{-2}\frac{F^2}{F^2+1.15^2} + 5.58\frac{F^2}{F^2+75.6^2} + 3.90\times10^{-5}\,F^2 \tag{5}$$

where F is the frequency in kilohertz, i.e., $F = f/(1\text{ kHz})$.

Alternatively, converting to decibels

$$\frac{\alpha_{\text{water}}}{\text{dB}\cdot\text{km}^{-1}} = 0.1216\frac{F^2}{F^2+1.15^2} + 48.47\frac{F^2}{F^2+75.6^2} + 3.874\times10^{-4}\,F^2. \tag{6}$$

The sea surface and seabed are both smooth (zero roughness). The sediment is a fluid (zero shear speed). The symbol α represents the imaginary part of the complex wave number

$$k = \frac{2\pi f}{c} + i\alpha. \tag{7}$$

TABLE VIII
SUMMARY OF WORKSHOP PROBLEMS

#	Name	Source	Scatter in airgun position (in x direction)	Scatter in airgun position (in y and z directions)	Absorption in water
1	Lossless	S1	0	0	Off
2	Baseline	S1	0	0	On
3	Line source	S2	0	0	On
4	Full array	S3	0.25 m	0.5 m	On

V. PROBLEM SPECIFICATION

A. List of Test Problems

A list of the test problems is shown in Table VIII.

Authors were encouraged to evaluate the following properties of the source (see Table IX):

1) source waveform s (known alternatively as the "notional source signature" [11], [12]) of individual airguns versus time t;
2) source spectrum S of individual airguns versus frequency f;
3) surface-affected source waveform s' of sources S1, S2, and S3 versus time t;
4) surface-affected source spectrum S' of sources S1, S2, and S3 versus frequency f.

Authors were encouraged to evaluate the following properties of the sound field (see Table X):

1) sound pressure p and sound particle acceleration $\boldsymbol{a}$ versus time t;
2) sound pressure exposure level $L_{E,p,\text{ddec}}$ and sound particle acceleration exposure level $L_{E,a,\text{ddec}}$ in decidecade frequency bands versus center frequency f_c;
3) sound pressure exposure level $L_{E,p,\text{ddec}}$ and sound particle acceleration exposure level $L_{E,a,\text{ddec}}$ in decidecade frequency bands versus range r;
4) propagation loss and broadband sound exposure level versus range r.

B. Decidecade Frequency Bands

One-tenth decade (decidecade) frequency bands are calculated according to IEC 61260-1:2014 [21] (IEC 61260-1:2014 refers to decidecade bands as "one-third octave" bands). The center frequency for decidecade band with index n is given by

$$f_c = 1000\ \cdot 10^{n/10}\ \text{Hz}. \tag{8}$$

The band-edge frequencies are one-twentieth of a decade above and below the center frequency

$$f_{\min} = 10^{-1/20}\ f_c \tag{9}$$

$$f_{\max} = 10^{+1/20}\ f_c \tag{10}$$

such that the decidecade band whose center frequency is 1 kHz ($n = 0$) spans the frequency range 0.89125–1.1220 kHz. Selected decidecade bands referred to later in this paper are listed in Table XI.

VI. CLOSING REMARKS

We conclude with some remarks on the realism of the test cases and the accuracy of the source waveform provided.

A. Realism of the Environment

Certain features of shallow water sound propagation are deliberately simplified to encourage modelers to focus on the source signature (calculation of $s(t)$ and $S(f)$) and the source-propagation model interface

TABLE IX
SUMMARY OF OUTPUT OPTIONS (SOURCE PROPERTIES)

Quantity	Unit	Where (θ, ϕ)	Notes
Source waveform **symbol** : $s(t)$	Pa m	-	Source waveform is defined by [3].
Source spectrum **symbol** : $S(f)$	Pa m/Hz	-	Source spectrum is defined by [3] as the Fourier transform [22] of the source waveform. See notes.
Surface-affected source waveform $s'(t)$ **synonym** : far-field signature	Pa m	θ = 20° (below horizontal) ϕ = 0, 90°, 180°, 270° and θ = 90° (independent of ϕ)	Surface-affected source waveform is defined by [3].
Surface-affected source spectrum $S'(f)$	Pa m/Hz	θ = 20° (below horizontal) ϕ = 0, 90°, 180°, 270° and θ = 90° (independent of ϕ)	Surface-affected source spectrum is defined by [3] as the Fourier transform of the surface-affected source waveform. See notes.

Notes: 1) For complex spectra, the magnitude and argument of a complex quantity $Z(f)$ are needed to provide a full description. In principle, this can be achieved by plotting the magnitude $A(f) = |Z(f)|$ and phase $\psi = \arg(Z)$ as a function of frequency, in the range (say) 0–7 kHz. In practice, the phase varies very quickly, and it is more practical to plot its derivative. Suggested plots are $A(f)$ and $d\psi/df$ on a logarithmic frequency axis from 1 to 10 kHz, and the phase itself $\psi(f)$ from 0 to 100 Hz.
2) Padding with zeros in the time domain up to about 10 s ensures a smooth spectrum at low frequency.

TABLE X
SUMMARY OF OUTPUT OPTIONS (SOUND FIELD PROPERTIES)

Quantity	Unit	Where (z, r; ϕ)	Notes[a]
Sound pressure vs time $p(t)$	Pa	z = [5, 15*, 25, 35, 45] m r = 0, 3 m, 30 m, 300 m, 3 km, 30 km ϕ = 0, 90°, 180°, 270°	
Sound particle acceleration vs time $\boldsymbol{a}(t)$	m/s^2	z = [5, 15*, 25, 35, 45] m r = 0, 3 m, 30 m, 300 m, 3 km, 30 km ϕ = 0, 90°, 180°, 270°	x, y and z components
Time-integrated squared sound pressure level vs center frequency $L_{E,p,\mathrm{ddec}}(f_c)$ **Reference value**: 1 μPa^2 s	dB	z = [5, 15*, 25, 35, 45] m r = [0, 3, 30, 300*, 3000*, 30 000*] m ϕ = 0, 90°, 180°, 270° + rose[b] (optional)	In decidecade bands
Time-integrated squared sound particle acceleration level vs center frequency $L_{E,a,\mathrm{ddec}}(f_c)$ **Reference value**: 1 (μm/s^2)^2 s	dB	z = [5, 15*, 25, 35, 45] m r = [0, 3, 30, 300*, 3000*, 30 000*] m ϕ = 0, 90°, 180°, 270° + rose (optional)	In decidecade bands
Time-integrated squared sound pressure level vs range $L_{E,p,\mathrm{ddec}}(r)$ **synonyms**: sound exposure level; sound pressure exposure level **Reference value**: 1 μPa^2 s	dB	z = [5, 15*, 25, 35, 45] m ranges of interest: 0–30 km ϕ = 0, 90°, 180°, 270° + rose (optional)	In decidecade bands centered at[c] f = [10, 100*, 501, 1000*, 1995, 6310, 10000] Hz
Time-integrated squared sound particle acceleration level vs range $L_{E,a,\mathrm{ddec}}(r)$ **Reference value**: 1 (μm/s^2)^2 s	dB	z = [5, 15*, 25, 35, 45] m ranges of interest: 0–30 km ϕ = 0, 90°, 180°, 270° + rose (optional)	In decidecade bands centered at f = [10, 100*, 501, 1000*, 1995, 6310, 10000] Hz
Propagation loss vs range $N_{\mathrm{PL}}(r)$ **Reference value**: 1 m^2	dB	z = [5, 15*, 25, 35, 45] m ranges of interest: 0–30 km	For a point monopole source at depth 5 m For f = [10, 30, 100, 500*, 1000, 2000*, 7000*, 10000] Hz[d]

[a] Asterisks indicate preferred values.
[b] A "rose" is a graph of a quantity (in this case sound pressure exposure level) versus ϕ in polar coordinates.
[c] Frequencies are rounded to the nearest integer in hertz. Indices are $n = [-20, -10, -3, 0, +3, +8, +10]$.
[d] Frequencies indicated by an asterisk correspond to twice the original WMW frequencies of 250, 1000, and 3500 Hz. This ensures that in the absence of absorption in water, the problem scales precisely with the water depth.

TABLE XI
DECIDECADE FREQUENCY BANDS FOR SELECTED INDEX n

Index	Minimum frequency / Hz	Center frequency / Hz	Maximum frequency / Hz
−20	8.9125	10.000	11.220
−10	89.125	100.00	112.20
−3	446.68	501.19	562.34
0	891.25	1000.0	1122.0
3	1778.3	1995.3	2238.7
8	5623.4	6309.6	7079.5
10	8912.5	10000	11220

Note: Frequencies are rounded to five significant figures.

(calculation of sound pressure $p(t)$ and sound particle acceleration $\boldsymbol{a}(t)$ given $s(t)$ or $S(f)$ as input). Examples of possible future improvements include incorporation of the following:

1) layering in the seabed [23];
2) shear waves in the seabed [24];
3) dispersion in the seabed [25];
4) roughness of the seabed or sea surface [26];
5) near-surface wind-generated bubbles [27].

B. Realism of the Source Description

Examples of possible future improvements taking into account the following:

1) the position of the nearest neighbor for spatial offsets, including statistical variations between pulses;
2) offsets in airgun firing times.

C. Accuracy of the Source Waveform

The source waveforms presented in this paper were calculated using Agora-2. Agora was chosen in preference to other source waveform models because it is a public domain code, developed by one of the authors (H. Ö. Sertlek) and available with a GNU General Public License from the Ocean Acoustics Library [9]. No claim is made on the accuracy of Agora relative to that of other airgun source waveform models used in this Special Issue, in the Dublin workshop [2], or anywhere else.

ACKNOWLEDGMENT

The authors would like to thank Dr. M. B. Halvorsen (CSA Ocean Sciences, Inc., Stuart, Florida) and Dr. K. D. Heaney (OASIS, Inc., Boone, NC, USA) for their comments on an earlier versions of this problem description, J. Janmaat for the use of his magic wand, and R. P. A. Dekeling (Netherlands Ministry of Infrastructure and the Environment, The Hague, The Netherlands) for his consistent and enthusiastic support throughout.

REFERENCES

[1] M. A. Ainslie, K. D. Heaney, and A. O. MacGillivray, "Guest editorial: Special Issue on Verification and Validation of Airgun Source Signature and Sound Propagation Models," *IEEE J. Ocean. Eng.*, vol. 44, no. 3, pp. 551–559, Jul. 2019.
[2] M. A. Ainslie *et al.*, "Verification of airgun sound field models for environmental impact assessment," in *Proc. Meetings Acoust.*, vol. 27, no. 1, 2016, Art. no. 070018.
[3] Underwater *Acoustics*—Terminology, ISO 18405:2017, 2017.
[4] IEEE Standard Letter Symbols for Units of Measurement (SI Units, Customary Inch-Pound Units, and Certain Other Units). (Revision of IEEE Std 260.1-1993), IEEE STD-260.1-2004, 2004.
[5] M. E. G. D. Colin *et al.*, "Definition and results of test cases for shipping sound maps," in *Proc. OCEANS Conf.*, Genoa, Italy, 2015, pp. 1–9.
[6] M. A. Ainslie, Ed., "Editorial: Validation of sonar performance assessment tools," in *Validation of Sonar Performance Assessment Tools: In Memory of David E Weston*. Cambridge, U.K.: Clare College, Apr. 2010, pp. 2–6.
[7] J. F. Parrish, "Air gun warmup," in *Proc. 55th Annu. SEG Meeting*, 1985, pp. 429–430.
[8] H. Ö. Sertlek and M. A. Ainslie, "Airgun source model (Agora): Its application for seismic surveys sound maps in the Dutch North Sea," in *Proc. Conf. Proc. UACE*, Platanias, Crete, Greece, 2015, pp. 439–446.
[9] "AGORA: Airgun Array Signature Model 2," Ocean Acoustics Library, 2018. [Online]. Available: https://oalib-acoustics.org/Sound%20and%20Marine%20Mammals/AGORA_version2.zip
[10] H. Ö. Sertlek, M. A. Ainslie, and R. M. Laws, "Agora source signatures for the International Airgun Modelling Workshop." [Online]. Available:http://dx.doi.org/10.21227/5081-yr65
[11] A. Ziolkowski, G. Parkes, L. Hatton, and T. Haugland, "The signature of an air gun array: Computation from near-field measurements including interactions," *Geophysics*, vol. 47, no. 10, pp. 1413–1421, 1982.
[12] G. E. Parkes, A. Ziolkowski, L. Hatton, and T. Haugland, "The signature of an air gun array: Computation from near-field measurements including interactions—Practical considerations," *Geophysics*, vol. 49, no. 2, pp. 105–111, 1984.
[13] R. Laws, M. Landrø, and L. Amundsen, "An experimental comparison of three direct methods of marine source signature estimation," *Geophysics*, vol. 46, no. 4, pp. 353–389, 1998.
[14] A. Ziolkowski, "A method for calculating the output pressure waveform from an air gun," *Geophys. J. Int.*, vol. 21, no. 2, pp. 137–161, 1970.
[15] R. M. Laws, L. Hatton, and M. Haartsen, "Computer modeling of clustered airguns," *First Break*, vol. 8, no. 9, pp. 331–338, 1990.
[16] A. O. MacGillivray, "Acoustic modelling study of seismic airgun noise in queen charlotte basin," M.Sc. thesis, School Earth Ocean Sci., Univ. Victoria, Victoria, BC, Canada, 2006.
[17] A. Ziolkowski and G. Metselaar, "The pressure wave field of an air gun array," in *Proc. SEG Annu. Meeting*, 1984, pp. 274–276.
[18] H. Ö. Sertlek and M. A. Ainslie, "A depth-dependent formula for shallow water propagation," *J. Acoust. Soc. Amer.*, vol. 136, no. 2, pp. 573–582, 2014.
[19] H. Ö. Sertlek, M. A. Ainslie, and K. D. Heaney, "Analytical and numerical propagation loss predictions for gradually range-dependent isospeed waveguides," *IEEE J. Ocean. Eng.*, 2018, doi: 10.1109/JOE.2018.2865640.
[20] M. A. Ainslie, *Principles of Sonar Performance Modeling*. Berlin, Germany: Springer, 2010.
[21] Electroacoustics—Octave-*Band* and *Fractional-Octave-Band Filters*—Part 1: Specifications, IEC 61260-1:2014, 2014.
[22] Quantities and Units—Part 2: Mathematical *Signs* and *Symbols* to *Be Used* in the *Natural Sciences* and *Technology*, ISO 80000-2:2009, 2009.
[23] E. L. Hamilton, "Geoacoustic modeling of the sea floor," *J. Acoust. Soc. Amer.*, vol. 68, no. 5, pp. 1313–1340, 1980.
[24] J. M. Hovem, M. D. Richardson, and R. D. Stoll, Eds., *Shear Waves in Marine Sediments*. New York, NY, USA: Springer, 2012.
[25] J.-X. Zhou, X.-Z. Zhang, and D. P. Knobles, "Low-frequency geoacoustic model for the effective properties of sandy seabottoms," *J. Acoust. Soc. Amer.*, vol. 125, no. 5, pp. 2847–2866, 2009.
[26] L. M. Brekhovskikh and Y. P. Lysanov, *Fundamentals of Ocean Acoustics*. New York, NY, USA: Springer, 2003.
[27] M. A. Ainslie, "Effect of wind-generated bubbles on fixed range acoustic attenuation in shallow water at 1–4 kHz," *J. Acoust. Soc. Amer.*, vol. 118, no. 6, pp. 3513–3523, 2005.

Michael A. Ainslie received the B.Sc. degree in physics from Imperial College London, London, U.K., in 1981, the MASt degree in mathematics from the University of Cambridge, Cambridge, U.K., in 2011, and the Ph.D. degree in seabed acoustics from the University of Southampton, Southampton, U.K., in 1991.

He is currently a Senior Scientist with JASCO Applied Sciences (Germany), Eschborn, Germany, and a Visiting Professor with the Institute of Sound and Vibration Research, University of Southampton. He is the author of the book *Principles of Sonar Performance Modeling* (Springer, 2010). His research interests include sonar performance modeling and effects of sound on aquatic life.

Dr. Ainslie is a Convenor of the ISO Working Group ISO/TC 43/SC 3/WG 2 (Underwater Acoustical Terminology) and a Member of the ANSI Working Group ANSI/S 3/WG73 (Bioacoustical Terminology).

Robert M. Laws received the B.Sc. degree in physics from Oxford University, Oxford, U.K., in 1976, and the Ph.D. degree in geophysics from Imperial College London, London, U.K., in 1991.

He worked in the field of marine seismic imaging for much of his career, including more than 20 years at Schlumberger's research laboratory in Cambridge, U.K. He is currently a Consultant on marine seismic sources. His Ph.D. dissertation was on the topic "modeling of oscillating airgun bubbles." In recent years, he has focused his attention on the impact of seismic sources on marine life, and he was a key player in the development of the E-source, a new design of airgun with a reduced environmental impact, and of the BASS marine seismic vibrator.

H. Özkan Sertlek received the B.Sc. degree in electronic engineering and the M.S. degree in underwater acoustic propagation from the Department of Electronic Engineering, Gebze Technical University, Gebze, Turkey, in 2006 and 2008, respectively, and the Ph.D. degree in bioacoustics from the University of Leiden, Leiden, The Netherlands, in 2016.

Between 2006 and 2011, he was a Researcher with the Technical Research Council of Turkey (TUBITAK). In summer 2009, he was a Research Fellow with NATO Undersea Research Centre. He is currently a Postdoctoral Researcher with Delft University of Technology, Delft, The Netherlands. His scientific interests include underwater acoustic propagation methods, sound mapping for the environmental risk assessment, and seismic sound source modeling.